Step-Terrace Morphology and Reactivity to C60 of the Fivefold i-Ag-In-Yb Surface

Peter John Nugent, Joe Smerdon, Ronan Mcgrath, Masahiko Shimoda, Can Cui, a Peter Tsai, Hem Raj Sharma

Step-Terrace Morphology and Reactivity to C_{60} of the Fivefold *i*-Ag-In-Yb Surface

Journal:	*Philosophical Magazine & Philosophical Magazine Letters*
Manuscript ID:	TPHM-10-May-0232
Journal Selection:	Philosophical Magazine
Date Submitted by the Author:	30-May-2010
Complete List of Authors:	Nugent, Peter; University of Liverpool, Physics Smerdon, Joe; University of Liverpool, Physics McGrath, Ronan; The University of Liverpool, Physics Shimoda, Masahiko; National Institue of Material Science Cui, Can; National Institue of Material Science Tsai, A; Tohoku University, National Institute for Materials Science Sharma, Hem; University of Liverpool, Physics
Keywords:	quasicrystals, surfaces
Keywords (user supplied):	Ag-In-Yb, C60, Scanning Tunneling Microscopy

Philosophical Magazine
Vol. 00, No. 00, 00 Month 200x, 1–7

RESEARCH ARTICLE

Step-Terrace Morphology and Reactivity to C_{60} of the Fivefold *i*-Ag-In-Yb Surface

P.J. Nugent[1*], J.A. Smerdon[1], R. McGrath[1], M. Shimoda[2], C. Cui[2], A.P. Tsai[2,3] and H.R. Sharma[1]

[1]*Surface Science Research Centre and Department of Physics, The University of Liverpool, Liverpool L69 3BX, United Kingdom*;
[2]*National Institute for Materials Science, 1-2-1 Sengen, Tsukuba, Ibaraki, 305-0047, Japan*;
[3]*Institute of Multidisciplinary Research for Advanced Materials, Tohoku University, Sendai, 980-8577, Japan*

()

The surface of the icosahedral *i*-Ag-In-Yb quasicrystal provides one of the first non Al-based aperiodic surfaces that is suitable for study under ultra high vacuum conditions. We present a scanning tunneling microscopy (STM) study of the fivefold surface of this new quasicrystal demonstrating detailed structure of the terraces and steps. The analysis of the autocorrelation functions of STM images at opposite bias polarities and of the in-plane structure of the bulk model of *i*-Cd-Yb, which is isostructural to *i*-Ag-In-Yb, reveals that the surface terminations occur at the centres of the rhombic triacontrahedral (RTH) clusters, that are the basic building blocks of this material. The study further confirms that the occupied electronic states are enhanced at Ag/In sites and unoccupied states are located on Yb sites. Step edges display a Fibonacci sequence of truncated clusters, which can be also explained in terms of the model structure. Occasionally, a single terrace is found to display different structures at negative bias, whereas the same terrace show a uniform structure at positive bias. Depositing C_{60} creates a disordered overlayer on the surface with no resulting FFT or LEED patterns.

Keywords: Quasicrystal; Ag-In-Yb; C60; Scanning Tunneling Microscopy; Autocorrelation; Fibonacci Sequence; Surface Morphology; Bias Dependence

1. Introduction

The discovery of the thermally stable binary icosahedral (*i*) quasicrystal, Cd-Yb [1], opened a new area of research in the field of aperiodic materials. Unlike previously discovered thermally stable quasicrystals, all of which are ternary, *i*-Cd-Yb is composed of only two materials, which has allowed for a full structural solution of an icosahedral quasicrystal [2]. The *i*-Cd-Yb quasicrystal, whose structure can be considered to be an aperiodic lattice of rhombic triacontrahedral (RTH) clusters, is structurally different from previously studied Al-based quasicrystals, which are formed from Mackay clusters [3]. Al-based quasicrystals display many interesting physical and electronic properties such as hardness, low surface friction and high electrical conductivity [4], and the *i*-Cd-Yb quasicrystal also displays un-

*Corresponding author. Email: p.nugent@liv.ac.uk

ISSN: 1478-6435 print/ISSN 1478-6443 online

DOI: 10.1080/1478643YYxxxxxxxx
http://www.informaworld.com

usual physical properties such as large electronic specific heat coefficients and high magnetoresistance [5–7].

The *i*-Cd-Yb quasicrystal is unsuitable for ultra high vacuum (UHV) study due to the high vapour pressure of Cd, which leads to evaporation on heat treatment, and as such it is difficult to prepare surfaces using the usual surface science methods of ion bombardment and annealing. This issue has been resolved by replacing Cd in this system with equal amounts of Ag and In. This new material, *i*-Ag-In-Yb, maintains the same electron to atom ratio of 2.0 and is isostructural to Cd-Yb, [8, 9] and Ag and In are stable in UHV, which allows the study of this quasicrystal in UHV environments.

In previous work, Sharma *et al.* [10, 11] succeeded in characterising the structure of the fivefold surface of *i*-Ag-In-Yb using scanning tunneling microscopy (STM), low energy electron diffraction (LEED) and reflection high energy electron diffraction (RHEED). In more recent work, the core levels and valence band structure of the same material have been characterised using x-ray photoelectron spectroscopy (XPS) [12] and ultraviolet photoelectron spectroscopy (UPS) [13]. With a combination of STM data of the fivefold *i*-Ag-In-Yb surface and the model structure of *i*-Cd-Yb, it has been possible to determine which bulk planes are responsible for surface terminations. Results indicate that surfaces terminate on the bulk planes which intersect the centre of the RTH clusters.

With the clean surface characterised and its structure understood, it is now possible to use this material as a substrate for thin film growth and adsorption of molecules. There is great interest in growing thin films using quasicrystals as templates and thus exploring the properties of two-dimensional single-element or molecular quasicrystalline structures [14, 15].

In this paper we present and characterise several structural features of the fivefold *i*-Ag-In-Yb surface that were not described in the previous publication [11]. In particular, we will focus on the step-terrace morphology studied by using new high resolution STM images. In addition, we will present a study on the adsorption of C_{60} on the same surface.

2. Experimental Details

The Bridgman method was used to produce a single grain sample of composition $Ag_{42}In_{42}Yb_{16}$ [8, 9, 16], which was cut perpendicular to the fivefold axis determined by Laue back-scattering. It was then mechanically polished using 6, 1 and 0.25 μm diamond paste. Atomically flat terraces were obtained through cycles of 2.5 KeV Ar^+ sputtering (30 - 60 minutes) at room temperature followed by annealing at 715 K (2 - 4 hrs) at a pressure of 1.4×10^{-10} mbar. Temperatures were monitored using an infra-red pyrometer set at an emissivity of 0.35.

STM experiments were performed in Ultra High Vacuum (UHV) using an Omicron variable temperature STM operating at room temperature. The stated bias refers to to the potential applied to the sample relative to the tip. C_{60} was deposited using a home built evaporator with a tungsten filament wrapped tightly around a Pyrex crucible containing C_{60} powder. The sample remained at room temperature during deposition. The evaporator was operated at temperatures of 485 to 495 K.

3. Results and Discussion

It was shown previously that the fivefold surface of *i*-Ag-In-Yb quasicrystal yields atomically flat terraces with fivefold symmetry [11]. The surface possesses step

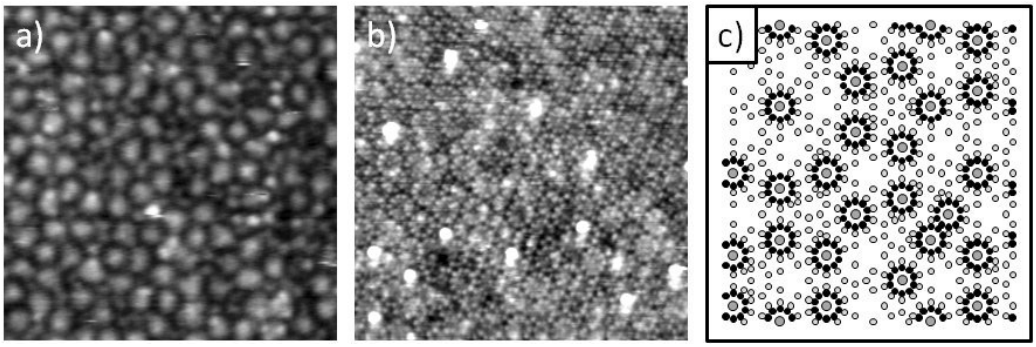

Figure 1. (a, b) High resolution STM images of the clean fivefold *i*-Ag-In-Yb surface taken at -0.81 V and 0.95 V respectively (30 nm × 30 nm). Image (b) has been enhanced using a fast Fourier filter (30 nm × 30 nm). (c) Surface termination plane taken from Cd-Yb model, with Cd featuring as black dots, and Yb as light grey dots. The plane intersects the middle of the RTH clusters, displayed as larger dark grey dots (20 nm × 20 nm).

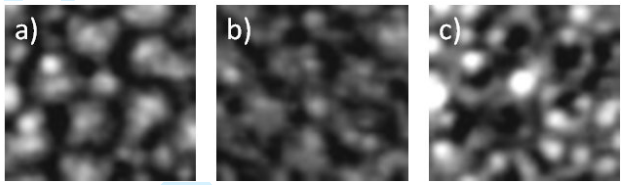

Figure 2. Highlighted feature of the clean surface of *i*-Ag-In-Yb at varying bias. (a, b, c) taken at -1.0 V, +0.1 V and +1.2V respectively.

heights of 0.28 ± 0.04, 0.58 ± 0.03 and 0.85 ± 0.05 nm, with respective percentage occurrences of 66%, 12% and 22%. These heights occur in the model structure as separations between atomic planes that intersect the centres of the RTH clusters.

STM images exhibit a strong bias dependence. Fig.1 (a) shows an STM image taken with a negative bias, which is composed of protrusions of size 1.30 ± 0.04 nm located at the vertices of pentagons of edge length 2.40 ± 0.15 nm. STM images can be compared directly to the in-plane structure intersecting the cluster centres shown in Fig.1 (c). The size of the protrusions corresponds to the diameter of the Cd ring, 1.27 nm. Fig.1 (b) shows an image obtained by applying a positive bias, which corresponds to unoccupied states, and has been taken from a different part of the surface. This image no longer displays protrusions and instead display rings of individual atoms. The rings have a diameter of 1.80 ± 0.09 nm, which corresponds to the diameter of 1.94 nm of the Yb rings from the model.

Fig.2 shows in greater detail the changes that occur as the bias is changed from negative to positive. These images feature a very common structural motif that exists on the surface. At negative bias, this feature appears as a pentagonal arrangement of protrusions. As the bias is changed, it is possible to resolve inside the protrusions. For instance, at +0.1 V bias, pentagons can be resolved at the vertices of the pentagonal arrangement of protrusions. This does not occur often, and can be related to the unknown distributions of Ag and In in the ring structure that a protrusion is constructed from. From the model structure of the approximant of *i*-Ag-In-Yb model, the surface layer is expected to be composed mostly of In [17], but the exact distribution of Ag and In in the ring is not known.

This is probably due to the density of states becoming localised to specific atoms, allowing for them to be resolved. As the bias is made more positive, these protrusions fade and are replaced by a pentagonal arrangement of rings (Fig.2 (c)).

Autocorrelation patterns from STM images indicate the presence of short and long range order by displaying the distances between recurring features that occur

in the images. Fig.3 (a, b) demonstrate autocorrelation pattern taken from negative and positive biased STM images respectively. The autocorrelation pattern from the negative image displays many rings of maxima with radii 2.3 nm, 3.8 nm, 6.1 nm and so on. These are related by 1, τ and τ^2 respectively, where τ is the golden mean, 1.618..., and confirm aperiodic order. The first maximum corresponds to the protrusion separations observed by STM.

The autocorrelation of a positive-bias STM image consists of smaller and more frequent rings of maxima. The first maximum occur at a radius of 0.6 nm which correspond to the atomic separation of Yb atoms, 0.6 nm. The radius of the second maxima at 1.1 nm originates from the next nearest neighbour separation of the Yb atoms, and is τ-related to the first maximum. The third maximum of 1.9 nm corresponds to the diameter of the Yb rings.

Autocorrelation patterns from the model structure are then compared to each other and the experimental results. Fig 3 (c, d) are autocorrelation patterns taken from the Cd-Yb model. Fig.3 (c) has been determined using the positions of the cluster centres which are associated with the positions of the protrusions. These have been modeled as a point source as opposed to larger objects that match the size of these protrusions, so that a clearer, sharper autocorrelation pattern is produced. The pattern agrees with that of the negative biased STM image shown in Fig.3 (a), apart from one feature. The first maximum on the theoretical autocorrelation pattern occurs at 1.4 nm which is smaller than the first maximum from the STM autocorrelation pattern by a factor of τ. This is because the model features a smaller cluster separation distance which is not resolved by STM. To compare the model structure to the positive biased autocorrelation, the Yb atom placements have been used. This produces a complex pattern similar to that of the experimental autocorrelation pattern, and as with the cluster centre position autocorrelation pattern, matches up well to the experimental data with maxima at similar positions. The positive bias autocorrelation patterns are a factor of τ^2 smaller than the negative bias autocorrelation patterns. This is consistent with the autocorrelation patterns from the model, and also consistent with fast Fourier transform (FFT) patterns obtained from the respective STM images (which are not shown).

Now we discuss the morphology of steps and terraces. At the edge of 0.28 nm high steps it is possible to observe protruding clusters from STM images taken at a negative bias. These protruding clusters can yield a Fibonacci sequence of L and S segments, extending for several tens of nanometers with a rare defect of a triple L sequence, as shown in Fig.4 (a). These L and S segments measure 4.24 ± 0.27 nm and 2.53 ± 0.22 nm respectively. These two lengths are τ-related, so that $L = \tau S$. L segments occur more often than S segments, with the ratio of occurrences also being related by τ. The Fibonacci sequence can be explained if the step-edge is parallel to the edge of the pentagon features observed in the substrate, which corresponds to high symmetry directions as shown in Fig.4 (b). These sequences are only observed on steps of the smallest height. This may be due to the larger step height being the product of two small step heights, causing a reconfiguration of clusters at the step edge to accommodate the height difference.

On several terraces imaged at negative bias, two different types of structure are observed as shown in Fig.5. One type displays a clearer configuration of protrusions than the other. The same area imaged with the same tip but at a positive bias shows a uniform structure as seen in Fig.5 (b). This may suggest that the non-uniformity encountered at a negative bias is related to an electronic effect.

We have investigated the reactivity of the surface by depositing C_{60} on the surface. Fig.6 (a) shows a sub-monolayer coverage with the area covered by roughly 10% of C_{60}. The protrusions observed on the image are 0.46 ± 0.04 nm or 0.65

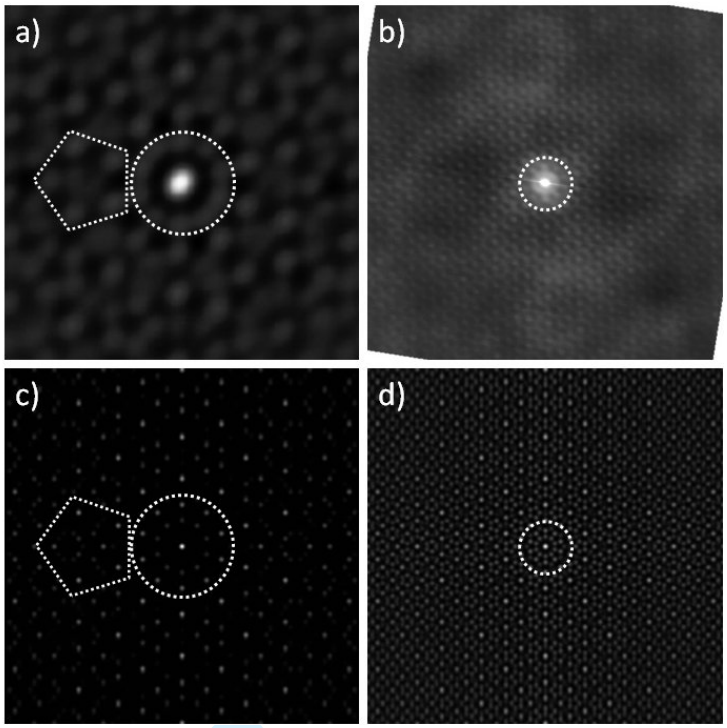

Figure 3. (a, b) are auto correlation patterns taken from negative and positive bias STM images respectively. These are accompanied by autocorrelation patterns taken from (c) the positions of clusters and (d) the positions of Yb atoms from the *i*-Cd-Yb model (20 nm × 20 nm).

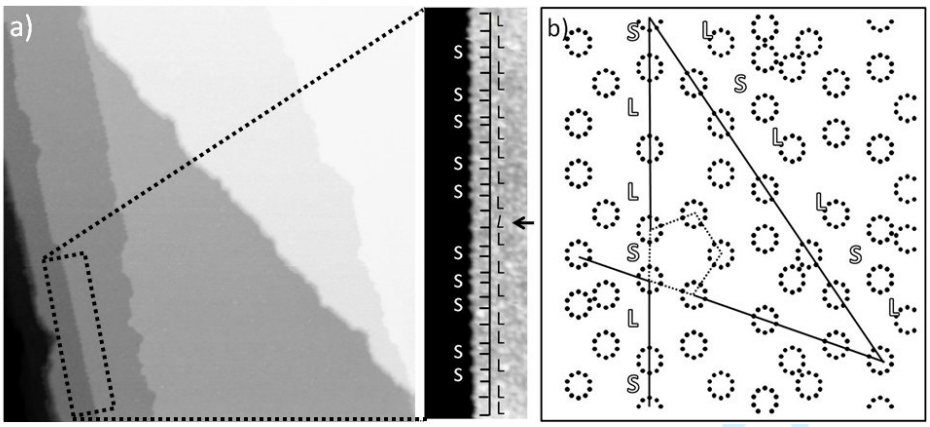

Figure 4. (a) Step terraced image from the clean fivefold *i*-Ag-In-Yb surface, with a step edge containing a 100 nm long sequence of protrusions (250 nm × 250 nm). The highlighted step edge on (a) is magnified on the right-hand-side. The indicated L section demonstrates a break in the sequence. (b) Section of the Cd-Yb model with only the Cd atoms displayed with several potential edge terminations marked by solid lines (20 nm × 20 nm).

± 0.04 nm in height, and 1.2 ± 0.1 nm in width, which are consistent with the dimensions of a C_{60} molecule. The smaller height corresponds to a C_{60} molecule adsorbing into the space between protrusions, while the larger is caused by a C_{60} molecule adsorbing on top of a protrusion, indicating no localised preferential adsorption site. Thresholding the image to remove the substrate contribution leaving just C_{60} yields an FFT without order indicating that C_{60} is adsorbed in a disordered fashion.

Depositing more than one monolayer of C_{60} shown in Fig.6 (b), leads to a disordered growth mode as evidenced by the FFT pattern. This coverage of C_{60}

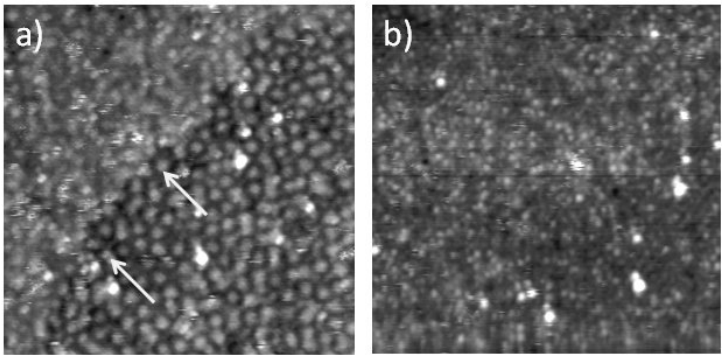

Figure 5. (a) STM image of the clean fivefold *i*-Ag-In-Yb surface taken at a bias of -1.0 V with an area of different surface structure highlighted. (b) Positive biased STM image of the same area taken at a bias of +1.0 V (100 nm × 100 nm).

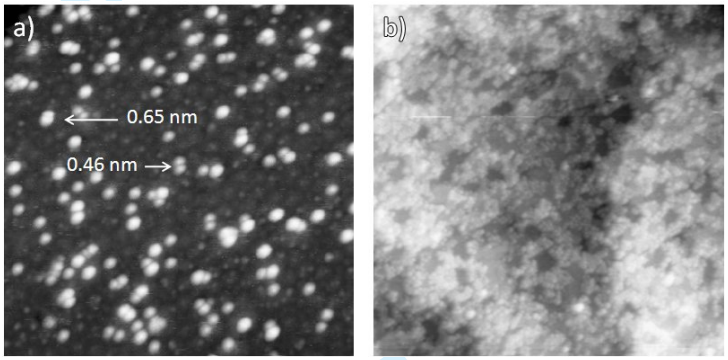

Figure 6. (a) Image of a 0.1 ML deposition of C_{60} on the fivefold *i*-Ag-In-Yb surface. Molecules have two different heights indicated by arrows (50 nm × 50 nm). (b) Image of > 1 ML of deposited C_{60} (100 nm × 100 nm).

suppresses the LEED spots from the substrate as surface order is destroyed.

4. Summary and Conclusions

Scanning tunneling microscopy has been successfully employed to characterise the fivefold *i*-Ag-In-Yb surface by identifying surface features and comparing these to the model structure of *i*-Cd-Yb. These surfaces intersect the centre of the RTH clusters that create the bulk of this material. The surface morphology imaged is dependent on the sample bias. At a negative bias, protrusions relating to Ag/In sites, which corresponds to the truncation of RTH cluster, while at a positive bias the Yb atoms are observed. This suggests that the occupied electronic states are enhanced at Ag/In sites and unoccupied states are located on Yb sites.

Truncated rhombic triacontrahedral clusters are visible at step-edges forming a Fibonacci sequence. This is expected from the model structure if the step is parallel to one of the high symmetry directions. Different structures have been observed on the same terrace when the sample is at a negative bias. This lack of uniformity is not observed at a positive bias, and may be an electronic effect.

Depositing C_{60} on the surface creates a disordered array of molecules, which provides no FFT pattern. Continued deposition leads to a disordered 3D growth mode.

References

[1] A. Tsai, J. Guo, E. Abe, H. Takakura and T. Sato, Nature 408 (2000) p.537–538.
[2] H. Takakura, C. Gómez, A. Yamamoto, M.D. Boissieu and A. Tsai, Nature Materials 6 (2007) p.58–63.
[3] M. Boudard, M. Boissieude , C. Janot, G. Heger, C. Beeli, H.U. Nissen, H. Vincent, R. Ibberson, M. Audier and J.M. Dubois, Journal of Physics: Condensed Matter 4 (1992) p.10149–10168.
[4] J.M. Dubois *Useful Quasicrystals*, World Scientific Publishing, 2005.
[5] Y. Muro, T. Sasakawa, T. Suemitsu, T. Takabatake, R. Tamura and S. Takeuchi, Jpn. J. Appl. Phys. 41 (2002) p.3787–3790.
[6] A. Pope, T. Tritt, R. Gagnon and J. Strom-Olsen, Appl. Phys. Lett. 76 (2001) p.2345–2347.
[7] R. Tamura, Y. Murao, S. Takeuchi, K. Tokiwa, T. Watanabe, T. Sato and A. Tsai, Jpn. J. Appl. Phys. 40 (2001) p.L912–L914.
[8] J. Guo and A. Tsai, Phil. Mag. Lett. 82 (2002) p.349–352.
[9] S. Ohhashi, J. Hasegawa, S. Takeuchi and A. Tsai, Phil. Mag. 87 (2007) p.3089–3094.
[10] H.R. Sharma, M. Shimoda, S. Ohhashi and A.P. Tsai, Phil. Mag. 87 (2007) p.2989–2994.
[11] H.R. Sharma, M. Shimoda, K. Sagisaka, H. Takakura, J.A. Smerdon, P.J. Nugent, R. McGrath, D. Fujita, S. Ohhashi and A.P. Tsai, Phys. Rev. B 80 (2009) p.121401–121406.
[12] P.J. Nugent, G. Simutis, V.R. Dhanak, M. Shimoda, R. McGrath, C. Cui, A.P. Tsai and H.R. Sharma, *Submitted* (2010).
[13] H.R. Sharma, G. Simutis, Dhanak, P.J. Nugent, C.Cui, M. Shimoda, R. McGrath, A.P. Tsai and Y. Ishii, Phys. Rev. B 81 (2010) p.104205–104205–7.
[14] H. Sharma, M.Shimoda and A. Tsai, Adv. Phys. 56 (2007) p.403–464.
[15] R. McGrath, J. Ledieu, E.J. Cox, S. Haq, C.J.J. R. D. Diehl, I. Fisher, A.R. Ross and T.A. Lograsso, J. Alloys Compounds 342 (2002) p.432–436.
[16] C. Cui and A.P. Tsai, J. Cryst. Growth 312 (2009) p.131–135.
[17] C. Gómez, private communication (2010).